Energy Performance of Alkali-Activated Cement-Based Concrete Buildings

Juan Pablo Gevaudan[1] and Wil V. Srubar III, Ph.D., A.M.ASCE[1*]

[1]Dept. of Civil, Environmental, and Architectural Engineering, Univ. of Colorado Boulder, 1111 Engineering Dr., ECOT 441 UCB 428, Boulder, CO 80309 (corresponding Author). E-mail: wsrubar@colorado.edu

Abstract

In the United States, the construction and operation of buildings account for approximately 40% of total energy consumption and total carbon dioxide emissions. In order to reduce these environmental impacts, truly net-zero energy buildings necessitate that both operational and embodied energy and carbon are offset through the combined use of high-performance building envelope materials and on-site renewable energy generation. Novel alkali-activated cement (AAC) concrete exhibits potential benefits such as lower thermal conductivity, equivalent compressive strength, and potentially lower environmental footprint, which translate to reductions in the amount of concrete material and lower environmental impacts compared to ordinary portland cement (OPC) concrete. The objective of this work was to quantify and compare the potential embodied and operational energy savings associated with the use of slag-based AAC concrete in relation to conventional OPC concrete and OPC+10% slag concrete in commercial building envelopes. Two functional units were considered for comparison, namely (a) constant volume replacement and (b) constant R-value of external wall assemblies. Using the Department of Energy (DOE) reference building models for commercial buildings to provide a consistent baseline for comparison, operational energy was quantified using EnergyPlus, a whole-building energy modeling tool, while embodied energy was quantified via lifecycle assessment (LCA) using inventory data obtained from the literature. The results demonstrate that, while total operational energy savings potential were negligible, AAC concrete buildings exhibit consistent reductions in material quantities and, thus, total embodied energy across climate regions. In addition to energy savings potential, the results of this study highlight the necessity to consider embodied energy in addition to operational energy when calculating the total energy consumption of truly net-zero energy buildings.

INTRODUCTION

Buildings are large energy consumers in the United States (US). According to the US Energy Information Administration, commercial and residential buildings consumed 40% of the nation's total end-use energy in 2015. As a result, low-energy buildings (LEBs) have been proposed as promising solutions to reduce energy consumption. To meet the operational energy reduction targets, the construction of LEBs often employ high embodied energy materials (Asif, Muneer, and Kelley 2007). Case studies on buildings built to different design criteria have shown that, while LEBs induce a net-benefit in total lifecycle energy demand, the total embodied the energy of buildings increases (Sartori and Hestnes 2007). Therefore, there is a growing need to focus not only on reducing operational energy but also on minimizing the embodied energy of materials used in high-performance buildings.

Alternative Cementitious Materials. As the most consumed material on Earth after water, ordinary portland cement (OPC) concrete is the third largest consumer of primary energy of all building materials and largest contributor of CO_2 emissions, which has prompted the development of alkali-activated cement (AAC) binders as eco-friendly alternatives to OPC (Zabalza Bribian, Valero Capilla, and Aranda Uson 2011). AAC binders are synthesized by dissolving an aluminosilicate material (e.g., metakaolin, fly ash) with (a) highly alkaline solutions (e.g., sodium hydroxide, potassium hydroxide) and (b) soluble silicates (e.g., sodium silicate). This dissolution reaction allows the aluminosilicates to restructure into a highly disorganized 3D inorganic polymer gel with cementitious properties. Resulting AAC concretes have exhibited lower (80-97%) carbon emissions associated with their production (McLellan et al. 2011; Duxson et al. 2007). However, the aluminosilicate source location, energy source and mode of transportation used throughout the manufacturing process of ACCs can have a significant effect on total energy and total CO_2 emissions. A recent Australian-based study compared transportation distances of different precursors for the production of AAC concrete and found that AACs can provide 44-64% reductions in greenhouse gas emissions (McLellan et al. 2011). According to the study, taking into account the transportation of the different raw materials, conventional OPC concrete mixtures produced approximately 333 kg-$CO_{2\text{-}}$e/m^3; OPC + 27% slag (as a cement replacement) concrete produced 212 kg-$CO_{2\text{-}}$e/m^3 and slag-based AAC concrete produced 201 kg-$CO_{2\text{-}}$e/m^3. The resulting reductions in carbon emissions are approximately 16% and 40% for both OPC + 27% slag and AAC concrete, respectively. Notably, transportation is one of the most significant factors affecting the carbon emissions associated with the productions of AACs. For example, emission increase by 20% with an increase of 50% in transportation distance from the raw material source (McLellan et al. 2011). Therefore, based on values from the literature, more realistic potential savings associated with using slag-based ACC is approximately 40% reduction in CO_2 emissions.

Thermal performance of materials. Thermal conductivity (*k*) is the main thermophysical material property in external wall assemblies that impacts the operational energy use of buildings. Thermal conductivity is the capacity of a material to conduct heat and is defined by the ratio of the flux of heat to the temperature gradient (Howlader et al. 2012). Recent studies on building envelope materials demonstrate the pivotal role of thermal conductivity in affecting the energy performance of building envelopes (Long and Ye 2016). Low thermal conductivity values can achieve heating and cooling building load reductions via decreased heat flow through the building envelope. For example, adobe (low thermal conductivity) in residential buildings has been shown to achieve 41.5% to 56.3% reductions in heating and cooling loads when compared to concrete brick houses in the same climate (Binici et al. 2007).

AAC concretes have also exhibited enhanced thermal properties, such as lower thermal conductivity, compared to OPC concretes. These enhanced thermal properties ultimately depend on the mixture proportioning and cement chemistry of the AAC mixture. Despite these thermal benefits, to the authors' knowledge, little to no studies have systematically analyzed potential operational and embodied energy impacts associated with the use of novel alkali-activated cement (AAC) concretes in comparison to OPC concrete in a building envelope application. The lack of reliable, methodically acquired data on the thermo-physical properties of AAC concrete has been a primary limiting factor in simulating the operational energy performance of these novel materials.

The aim of this paper was to provide an initial estimate of building operational and embodied energy benefits, if any, due to the use of AAC-based concrete in lieu of OPC-based concrete in a commercial building envelope application. Specifically, this study explores both operational energy (quantified *via* whole building energy simulation) and embodied energy (quantified *via* lifecycle assessment) impacts of three different concrete materials: (1) conventional OPC concrete; (2) OPC concrete with 10% blast furnace slag (as replacement for OPC); and (3) slag-based AAC concrete in an envelope of a medium-sized office building in different US climates.

METHODOLOGY

Operational energy analysis. For this study, two operational energy analyses were performed. These analyses were based on two functional units for comparison, namely (1) constant material volume and (2) constant R-value of the concrete wall assembly. The material thickness of OPC- and AAC-based concrete elements was held constant (0.2 m) in the first analysis to approximate real-life structural constraints. R-value was held constant in the second analysis (0.1 m^2-K/W) to simulate a case in which the structural considerations of a building could be neglected to explore the maximum potential embodied energy savings associated with decreased material use.

Thermo-physical material properties. First, necessary thermophysical data for OPC and AAC concrete materials were obtained from literature and/or approximated based on previous studies (Kim et al. 2003; Bentz et al. 2011). Lack of explicit investigations on the thermal performance of novel AAC-based materials necessitated the following assumptions:

- Thermal conductivity of slag-based AAC paste was approximated based on similar cement chemistry (Si:Al = 2, M^+:Al > 1) of metakaolin-based AACs at dry conditions (Kamseu et al. 2012).
- Thermal conductivity of slag-based AAC paste (average pore size: 18 nm, cumulative pore volume: 271.07 mm^3/g) was converted to concrete using empirical relations from previous relevant literature (Kim et al. 2003).

- Heat capacity was calculated by a simple rule of mixtures from the corresponding slag-based concrete mix design.
- Validation of previous assumptions was performed by calculating the thermal conductivity of OPC + 10% slag and comparing to the actual reported value in literature. Results show that calculated value is within 1% of the actual value of the concrete material.

Three parameters are needed to specify the building envelope materials impact on the operational of the building: density (ρ), heat capacity (C_p), and thermal conductivity (k). **Table 1** summarizes the thermal properties obtained for OPC and AACs. As seen in **Table 1**, AACs exhibit, on average, lower thermal conductivity and higher heat capacity than OPC mixtures.

Table 1. EnergyPlus modeling parameters for OPC, OPC + 10% slag, and AAC concretes of comparable compressive strengths (> 36 MPa)

Concrete	Density, ρ (kg/m^3)	Thermal Conductivity, k (W/m-K)	Heat Capacity, C_p (J/kg-K)
OPC	2317	2.00	704*
OPC + 10% Slag	2334	1.66	707
Slag-based AAC	2232	1.12*	739*

*Calculated values from (Kim et al. 2003, De Schutter and Taerwe 1995).

Building energy model information. Building energy models were adapted from the Department of Energy (DOE) commercial reference building models (ASHRAE 90.1-2013) to provide a consistent baseline for comparison and analyzed in EnergyPlus, a whole building energy modeling tool. OpenStudio 1.12.0, a simulation tool developed by the National Renewable Energy Laboratory, was utilized for model visualization and modifications of the EnergyPlus modeling file. This tool was selected based on modeling speed, ease of output definition, and ease of ability to change material properties from reference building models.

The DOE reference medium-sized office building (**Figure 1**) was selected from the 1980-2004 reference database. The building consists of a three-story building with a total floor area of 4982 meters squared. The window-to-wall ratio at each orientation is 33% and the windows modeled are simple glazing systems with a solar heat gain coefficient (SHGC) of 0.25 and an overall heat transfer coefficient (U-value) of 1.22. One notable limitation of the whole building energy modeling approach used herein is the absence of independent structural systems within the energy model that could potentially allow concrete materials to have a greater impact on the operational energy of the building.

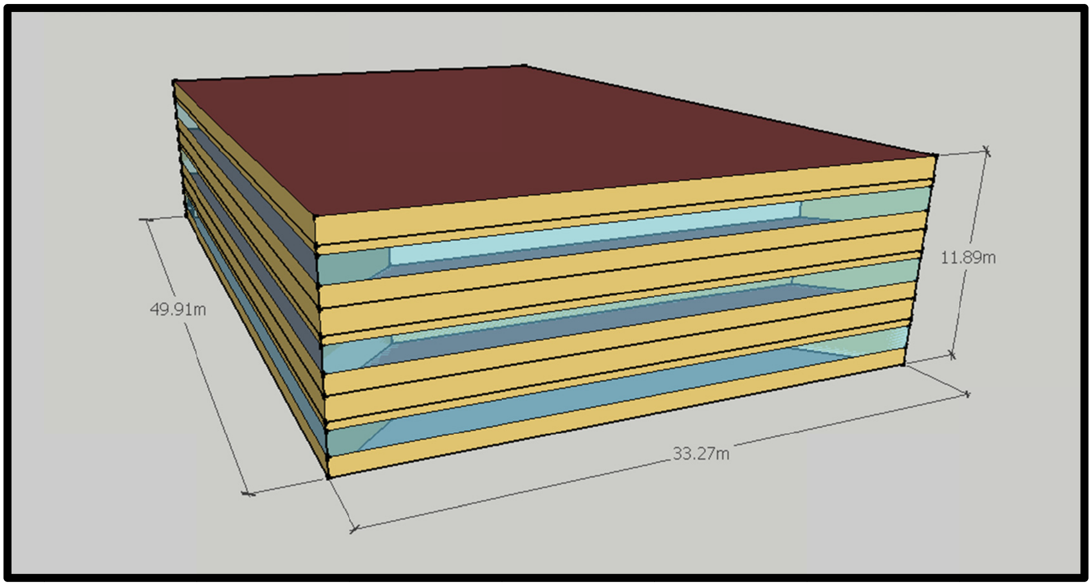

Figure 1. DOE medium-sized office building characteristics.

Two functional units were considered for the analysis, namely ***constant volume,*** and ***constant R-value***. For the constant volume analysis, the external wall assemblies included a concrete layer (0.20 m) to account for concrete material in a wall cavity in the building envelope. For the constant R-value analysis, the thicknesses of the OPC, OPC+10% slag, and AAC concrete were varied to obtain a constant R-value (0.1 m^2-K/W). The resulting thickness and R-values for each operational energy (OE) simulation are shown in **Table 2**.

Building energy simulations were run for a DOE medium-sized office building in nine (9) different US locations and climates, namely a Hot-Humid (Miami, FL- 1A), Hot-Dry (Phoenix, AZ- 2B), Mild-Marine (San Francisco, CA- 3C), Mild-Humid (Baltimore, MD- 4A), Mild-Dry (Albuquerque, NM- 4B), Cold-Humid (Chicago, IL- 5A), Cold-Dry (Denver, CO- 5B), Very Cold-Dry (Duluth, MN- 7A), and Extremely Cold-Dry (Fairbanks, AK- 8A) to compare the effect of location and climate on the energy performances of OPC, OPC+10% slag, and AAC concrete buildings.

Table 2. Thicknesses and R-values of concrete elements in the wall assembly.

Modeling Parameter	OPC Concrete	OPC+10% Slag Concrete	AAC Slag Concrete
OE/EE Comparison 1: Constant Volume Analysis			
Thickness (m)	0.20	0.20	0.20
R-Value (m^2-K/W)	0.10	0.12	0.18
OE/EE Comparison 2: Constant R-Value Analysis			
Thickness (m)	0.20	0.17	0.11
R-Value (m^2-K/W)	0.10	0.10	0.10

Embodied energy analysis. The goal of the lifecycle assessment (LCA) conducted in this study was to quantify the total embodied energy (EE) of OPC-, OPC+10% slag, and AAC-based concrete in a building wall assembly. The scope of the LCA included two functional units (described below) was a cradle-to-gate analysis of the volume of concrete material required for each energy simulation. Embodied carbon coefficients account for the transportation of hypothetical cast-in-place concrete applications. This assumption is valid since slag-based AAC concretes have been shown to exhibit satisfactory, fresh-state properties comparable with OPC *via* the use of admixtures (Bakharev, Sanjayan, and Cheng 2000). The data used are specific to Australia and include transportation from actual material sources. The authors recognize the limitations of using these data herein as a proxy and plan to complete a more robust lifecycle assessment for location-specific applications in follow-up analyses. The inventory of embodied energy coefficients used in the analysis is shown in **Table 3**.

Similar to the operational energy analysis, the functional unit used in the first analysis was a constant-volume unit, in which the total material thickness for each concrete assembly was held constant (0.20 m). Thus, the total volume of the material was held constant (270 m^3). The functional unit used in the second analysis was a constant R-value, in which the total volume of each concrete material was based on the thickness required for each material to obtain an R-value of 0.1 m^2-K/W (see **Table 2**). The variable thicknesses resulted in concrete volumes of 270 m^3, 220 m^3, and 150 m^3, for OPC, OPC+10% slag, and slag-based AAC concrete, respectively. Embodied energy coefficients were taken from published literature values for embodied carbon of OPC, OPC+10% slag, and slag-based AAC concrete on a per-mass basis.

Table 3. Embodied carbon and energy coefficients for OPC and AAC concretes, assuming 1 kg CO_2 = 5.12 MJ. (McLellan et al. 2011a)

Concrete	Embodied Carbon (kg CO_2/m^3)	Embodied Energy (MJ/m^3)
OPC	333	1705
OPC + 10% Slag	288*	1475*
Slag-based AAC	201	1029

*Interpolated.

RESULTS AND DISCUSSION

Operational Energy: Constant Volume. The results of the constant-volume operational energy simulations are shown in **Figure 2**. The results demonstrate that each concrete assembly exhibited similar operational energy performances. This result is attributable to the similar, albeit different, thermal properties of the concrete materials. As previously discussed, OPC+10% slag and slag-based AAC concretes exhibit improvements on insulation properties of OPC concrete (see **Table 2**) equal to a 17% and 44% reduction in thermal conductivity values, which result in 20% and 79% increase in R-value, respectively, when compared to conventional OPC concrete. Previous research has shown that thermal conductivity values decrease as more slag is incorporated into OPC concrete mixes. Lower conductivity values are likely due to an increase in amorphous silica, which is a poor thermal conductor (Xu and Chung 2000). Consequently, the external wall assembly's R-value is improved by 2% with the use of AAC concrete due to a 0.20-meter-thick concrete layer in the building envelope construction. The minimal improvement in the external wall assembly's R-value has marginal implications for the building operational energy.

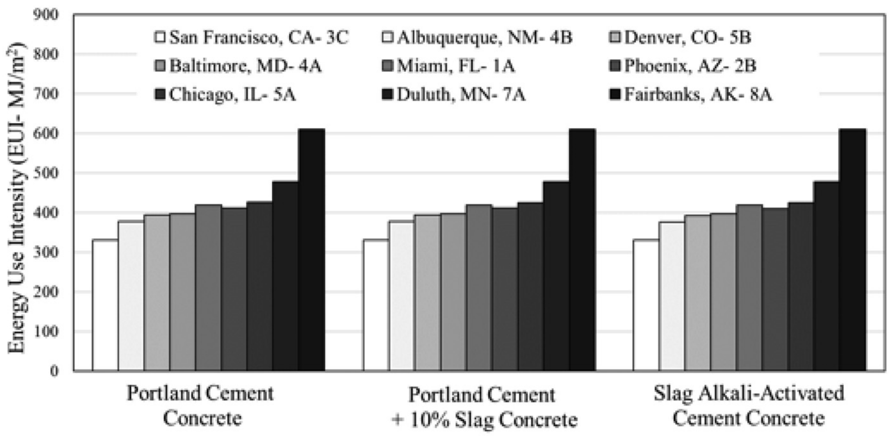

Figure 2. Variations in energy use intensity (EUI) across different climates for different concrete materials (Functional Unit: Constant Volume).

The thermal conductivity of concrete materials is influenced by both composition and porosity (cumulative pore volume and pore size distribution). However, the literature relating thermal conductivity to porosity and pore size distribution is highly fragmented. Recent studies demonstrate lower thermal conductivity values in concrete materials with the same porosity but with increased average pore size (Ropelewski and Neufeld 1999). Since pore sizes above 100 microns permit convection to affect thermal conductivity (Živcová et al. 2009), low thermal conductivity values, the authors argue, are due to greater convection inside pores above 100 microns in size. Small nano-sized pores in ceramic materials of the same porosity, however, have also been demonstrated to lower thermal conductivity. The phenomenon can be explained by a reduction in mean distance between adjacent pores with a smaller average pore size in ceramic materials with identical porosities (Sumirat, Ando, and Shimamura 2006). As a result, the authors argue, heat is transmitted less effectively due to the interference of random nano-sized pores (Loeb 1954; Francl and Kingery 1954). Experiments with increased porosity (and equal average pore size) demonstrate a negligible increase in thermal conductivity (Ropelewski and Neufeld 1999). The general consensus, therefore, is that thermal conductivity decreases with the increase of porosity, but this depends on the pore size distribution (Kamseu et al. 2012). It has also been shown that the extent of polymerization in AACs affects the final porosity and pore size distribution (Kamseu et al. 2012). In conclusion, the material values used in this simulation are specific to one specific slag-based AAC concrete. More explicit investigations on composition and porosity will allow the development of a general model to account for a greater range of AAC concrete materials.

In addition, the effect of climate on the energy savings (EUI, electricity and natural gas consumption) is minimal, yet increases in relation to heating building loads and humid climates. Replacement of OPC concrete with AAC concrete in medium-sized office buildings resulted in higher energy reductions across different climates compared to the OPC+10% slag cement concrete, as seen in **Table 4**. The maximum EUI improvement is observed in the extremely cold and dry climate of Fairbanks, Alaska (0.128%) when AAC concrete is used. The observed energy reductions in EUI are due to savings in electricity and natural gas consumption of buildings, see **Table 4**. While trivial, the results presented in both **Figure 2** and **Table 4** demonstrate that alternative cementitious materials exhibit equivalent thermal performances to conventional OPC – a finding that has not yet been reported in the literature. The superior performance of low thermally conductive materials in cold (5-8) and humid climates (A), when compared to hot/mild (1-4) and dry (B), while minimal, can be further diminished by the presence of climatic moisture.

Table 4. Comparison between OPC concrete replacement by OPC + 10% slag and slag-based AAC concrete in wall assemblies of medium-sized office buildings (Functional Unit: Constant Volume).

Concrete	Energy Use Intensity (EUI) (% reduction)	Electricity Consumption (% reduction)	Natural Gas Consumption (% reduction)
OPC + 10% Slag			
Miami, FL- 1A	0.01%	0.01%	0.00%
Phoenix, AZ- 2B	0.01%	0.01%	0.00%
San Francisco, CA- 3C	0.01%	0.01%	0.00%
Baltimore, MD- 4A	0.02%	0.02%	0.00%
Albuquerque, NM- 4B	0.01%	0.01%	0.00%
Chicago, IL- 5A	0.02%	0.02%	0.04%
Denver, CO- 5B	0.02%	0.02%	0.02%
Duluth, MN- 7A	0.03%	0.02%	0.02%
Fairbanks, AK- 8A	0.04%	0.04%	0.07%
Slag-based AAC			
Miami, FL- 1A	0.02%	0.02%	0.00%
Phoenix, AZ- 2B	0.05%	0.05%	0.00%
San Francisco, CA- 3C	0.02%	0.02%	0.00%
Baltimore, MD- 4A	0.06%	0.06%	0.05%
Albuquerque, NM- 4B	0.04%	0.05%	0.00%
Chicago, IL- 5A	0.07%	0.07%	0.09%
Denver, CO- 5B	0.06%	0.06%	0.08%
Duluth, MN- 7A	0.09%	0.09%	0.10%
Fairbanks, AK- 8A	0.13%	0.12%	0.17%

Non-consideration of moisture effects is a noted limitation of this initial study. Moisture distribution in the material due to humid climates affects the thermal conductivity of concrete materials. Building energy simulation results herein assume constant material thermophysical values despite real-case moisture distribution through the wall assembly. High Moisture content in concrete materials increases thermal conductivity and is a function of pore size distribution, porosity, exposure, and environmental conditions (i.e., humidity). Studies on ceramics have revealed that water absorption potential can be related to porosity and pore size distribution (Calabria, Vasconcelos, and Boccaccini 2009). Studies on these materials show that at similar porosities and bigger pore sizes (40-50 nm) there is a decrease in water absorption potential (Okada et al. 2009). Moreover, water absorption further decreases when pore size is maintained, but porosity decreases (0.39-0.35 ml/g). AAC concrete materials demonstrate two mechanisms for water absorption: (i) chemical fixation and (ii) physical absorption. Chemical fixation of atmospheric water and air is predominant and more important in the case of specimens with high Si/Al molar ratio (Kamseu et al. 2012). AAC concretes with a low silicon content have a low capacity to chemically fix atmospheric water (i.e., humidity), since the active sites with silica are less numerous. (Kamseu et al. 2012). In conclusion, high water absorption from highly humid climates by any concrete material can increase the thermal conductivity, thus, affecting potential energy costs and savings.

Embodied Energy: Constant Volume. Despite no impacts on operational energy, the use of OPC+10% slag and slag-based AAC concrete corresponded to reductions in total embodied energy. **Figure 3a** shows the embodied energy of the three concrete building assemblies assuming constant volume. The results demonstrate that the OPC+10% slag concrete building achieved a 13.5% reduction in total embodied energy compared to the OPC concrete building, while the slag-based AAC concrete achieved a 39.6% reduction. The results illustrate that the use of an AAC-based concrete can achieve embodied energy reductions up to 40% in a constant-volume scenario and not affect the operational energy performance of the building.

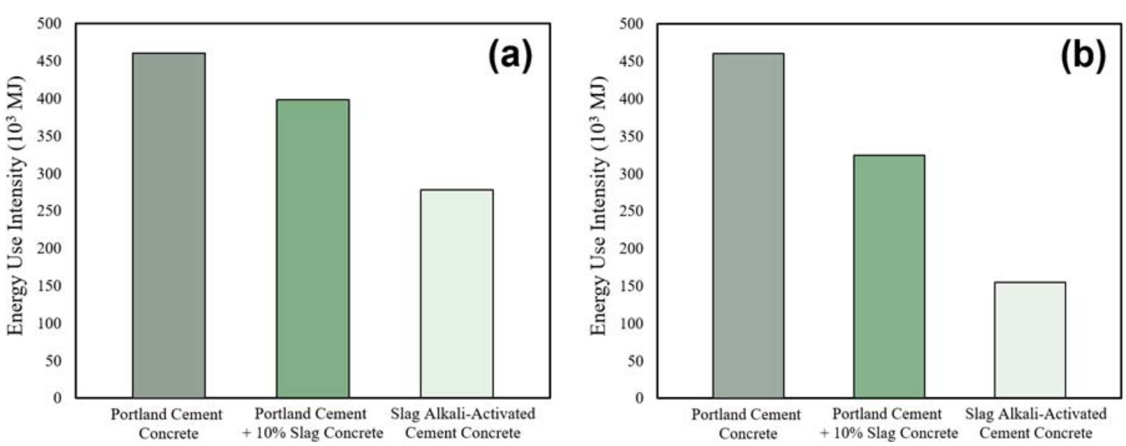

Figure 3. Embodied energy comparisons assuming (a) constant volume and (b) constant R-value. Data valid for all climates.

Operational and Embodied Energy: Constant R-Value. The operational energy performance of OPC, OPC+10% slag, and slag-based AAC concrete buildings was identical, yet their embodied energy shown in **Figure 3b** differed. As expected, the operational energy consumption is identical for each material investigated herein given a constant R-value assumption. However, as illustrated in **Figure 3b**, significant embodied energy reductions can be achieved by reducing the amount of material used in building envelopes. Reductions in material quantities were achievable by the OPC+10% slag and slag-based AAC concretes due to the better insulating properties of those concretes in comparison to OPC concrete. For the OPC+10% slag concrete and AAC concrete, improved thermal properties resulted in 17% and 44% reductions in material volume in comparison to OPC concrete, respectively. Along with the reduction in material quantities, the per-unit-volume embodied energy of AAC concrete is less than that of OPC concrete. These results illustrate that the use of an AAC-based concrete can achieve embodied energy reductions up to 66.5% in a constant R-value scenario and, similar to the constant volume scenario, not affect the operational energy performance of the building.

FUTURE WORK

Given limited data in the literature, the thermo-physical properties of AACs are, at present, poorly understood and necessitate further study. The body of knowledge on cement chemistry suggests that both alkali type and content, along with amorphous silica contents, impact the thermal conductivity of all cement-based materials. Generally, an increase in amorphous silica, as seen in OPC systems, decreases thermal conductivity. While the tailoring the amorphous silica contents of AAC-based systems is possible, realizing the true insulating potential of AACs requires more systematic experimental investigation.

Further consideration on the actual assembly systems in building energy models may provide a more detailed analysis of the role of alternative cement-based concrete materials in the operational energy impact of buildings. DOE reference building energy models are based on overall R-values of mass wall assembly constructions having a continuous layer of concrete. Continuous layer components do not necessarily account for different structural systems and their impact on building operational energy. For example, buildings employing external reinforced concrete structural components can be subject to energy-detrimental thermal bridges. Thermal bridging, influenced by the material's thermal conductivity values, can negatively impact the operational energy of buildings. Therefore, additional computational efforts should focus on improving energy simulation environments to account for these specialized and additional effects.

CONCLUSIONS

The aim of this paper was to provide a preliminary estimate of building operational and embodied energy impacts due to the use of alternative cements, namely (1) an ordinary portland cement (OPC) with 10% slag and (2) a slag-based AAC, in comparison to conventional OPC concrete for a building envelope application in different US climates. Two functional units were considered for comparison, namely (a) constant volume replacement and (b) constant R-value of external wall assemblies. Using the Department of Energy (DOE) reference building models for commercial buildings to provide a consistent baseline for comparison, operational energy was quantified *via* EnergyPlus, a whole-building energy modeling tool, while embodied energy was quantified *via* lifecycle assessment (LCA) using inventory data obtained from the literature.

The results demonstrate that, while constant volume and constant R-value comparisons were negligible in terms of total operational energy savings potential, the OPC+10% slag concrete and slag-based AAC concrete buildings exhibit consistent reductions in material quantities given their lower thermal conductivity. Lower material quantities resulted in total embodied energy reductions across different climate regions. The slag-based AAC concrete achieved maximum material quantity and embodied energy reductions of 44.4% and 66.5%, respectively, in the constant R-value scenario with no impact on the operational energy performance of the building. Although minor, replacements of OPC with slag in concrete are demonstrated to have little impact on the building's thermal performance when compared to OPC concrete.

While this preliminary study represents promising results for AAC concrete, a better understanding of the thermal benefits of AAC concrete in comparison to OPC concrete require future experimental and computational efforts. Experimentally, the thermo-physical properties of AACs (porosity, pore size distribution, moisture absorption, cement chemistry) have not yet been studied in detail and merits further investigation. Computationally, consideration of the actual structural system in building energy models may provide a more detailed analysis of the role alternative-cement concrete materials play in the operational energy impact of buildings.

ACKNOWLEDGMENTS

This research was made possible by the Department of Civil, Environmental, and Architectural Engineering, the College of Engineering and Applied Sciences, and the Sustainable Infrastructure Materials Laboratory (SIMLab) at the University of Colorado Boulder, with support from the National Science Foundation (Award No. CBET-1604457). This work represents the views of the authors and not necessarily those of the sponsors.

REFERENCES

Asif, M., T. Muneer, and R. Kelley. 2007. "Life Cycle Assessment: A Case Study of a Dwelling Home in Scotland." *Building and Environment* 42 (3): 1391–94. doi:10.1016/j.buildenv.2005.11.023.

Bakharev, T., J. G. Sanjayan, and Y. B. Cheng. 2000. "Effect of Admixtures on Properties of Alkali-Activated Slag Concrete." *Cement and Concrete Research* 30 (9): 1367–74. doi:10.1016/S0008-8846(00)00349-5.

Binici, Hanifi, Orhan Aksogan, Mehmet Nuri Bodur, Erhan Akca, and Selim Kapur. 2007. "Thermal Isolation and Mechanical Properties of Fibre Reinforced Mud Bricks as Wall Materials." *Construction and Building Materials* 21 (4): 901–6. doi:10.1016/j.conbuildmat.2005.11.004.

Calabria, Juliana A., Wander L. Vasconcelos, and Aldo R. Boccaccini. 2009. "Microstructure and Chemical Degradation of Adobe and Clay Bricks." *Ceramics International* 35 (2): 665–71. doi:10.1016/j.ceramint.2008.01.026.

De Schutter, G., and L. Taerwe. 1995. "Specific Heat and Thermal Diffusivity of Hardening Concrete." *Magazine of Concrete Research* 47 (172): 203–8. doi:10.1680/macr.1995.47.172.203.

Duxson, Peter, John L. Provis, Grant C. Lukey, and Jannie S.J. van Deventer. 2007. "The Role of Inorganic Polymer Technology in the Development of 'green Concrete.'" *Cement and Concrete Research* 37 (12): 1590–97. doi:10.1016/j.cemconres.2007.08.018.

Francl, J, and W. D. Kingery. 1954. "Thermal Conductivity: IX, Experimental Investigation of Effect of Porosity on Thermal Conductivity." *Journal of the American Ceramic Society* 37 (2): 99–107.

Howlader, Milon K, M H Rashid, Debashis Mallick, and Tozammel Haque. 2012. "Effects of Aggregate Types on Thermal Properties of Concrete." *ARPN Journal of Engineering and Applied Sciences* 7 (7): 900–906.

Kamseu, E., B. Ceron, H. Tobias, E. Leonelli, M. C. Bignozzi, A. Muscio, and A. Libbra. 2012. "Insulating Behavior of Metakaolin-Based Geopolymer Materials Assess with Heat Flux Meter and Laser Flash Techniques." *Journal of Thermal Analysis and Calorimetry* 108 (3): 1189–99. doi:10.1007/s10973-011-1798-9.

Kim, Kook-han, Sang-eun Jeon, Jin-keun Kim, and Sungchul Yang. 2003. "An Experimental Study on Thermal Conductivity of Concrete." *Cement and Concrete Research* 33: 363–71.

Loeb, Arthur L. 1954. "Thermal Conductivity: VII, A Theory of Thermal Conductivity of Porous Materials." *Journal of the American Ceramic Society* 37 (2): 96–99.

Long, Linshuang, and Hong Ye. 2016. "The Roles of Thermal Insulation and Heat Storage in the Energy Performance of the Wall Materials: A Simulation Study." *Scientific Reports* 6 (October 2015). Nature Publishing Group: 24181. doi:10.1038/srep24181.

McLellan, Benjamin C., Ross P. Williams, Janine Lay, Arie Van Riessen, and Glen D. Corder. 2011. "Costs and Carbon Emissions for Geopolymer Pastes in Comparison to Ordinary Portland Cement." *Journal of Cleaner Production* 19 (9–10). Elsevier Ltd: 1080–90. doi:10.1016/j.jclepro.2011.02.010.

Okada, Kiyoshi, Asami Ooyama, Toshihiro Isobe, Yoshikazu Kameshima, Akira Nakajima, and Kenneth J D MacKenzie. 2009. “Water Retention Properties of Porous Geopolymers for Use in Cooling Applications.” *Journal of the European Ceramic Society* 29 (10): 1917–23. doi:10.1016/j.jeurceramsoc.2008.11.006.

Ropelewski, Lawrence, and Ronald D. Neufeld. 1999. “Thermal Inertia Properties of Autoclaved Aerated Concrete.” *Journal of Energy Engineering* 125 (2): 59–75.

Sartori, I., and A. G. Hestnes. 2007. “Energy Use in the Life Cycle of Conventional and Low-Energy Buildings: A Review Article.” *Energy and Buildings* 39 (3): 249–57. doi:10.1016/j.enbuild.2006.07.001.

Sumirat, Iwan, Y. Ando, and S. Shimamura. 2006. “Theoretical Consideration of the Effect of Porosity on Thermal Conductivity of Porous Materials.” *Journal of Porous Materials* 13 (3): 439–43. doi:10.1007/s10934-006-8043-0.

Xu, Yunsheng, and D. D L Chung. 2000. “Cement of High Specific Heat and High Thermal Conductivity, Obtained by Using Silane and Silica Fume as Admixtures.” *Cement and Concrete Research* 30 (7): 1175–78. doi:10.1016/S0008-8846(00)00296-9.

Zabalza Bribian, Ignacio, Antonio Valero Capilla, and Alfonso Aranda Uson. 2011. “Life Cycle Assessment of Building Materials: Comparative Analysis of Energy and Environmental Impacts and Evaluation of the Eco-Efficiency Improvement Potential.” *Building and Environment* 46 (5). Elsevier Ltd: 1133–40. doi:10.1016/j.buildenv.2010.12.002.

Živcová, Zuzana, Eva Gregorová, Willi Pabst, David S. Smith, Aurélie Michot, and Céline Poulier. 2009. “Thermal Conductivity of Porous Alumina Ceramics Prepared Using Starch as a Pore-Forming Agent.” *Journal of the European Ceramic Society* 29 (3): 347–53. doi:10.1016/j.jeurceramsoc.2008.06.018.